

EVS27
Barcelona, Spain, November 17-20, 2013

Practical Field Weakening Current Vector Control Calculations for PMSM in Vehicle Applications

Tim Martin¹, Richard Burke

¹*Protean Electric Limited, Farnham, UK, tim.martin@proteanelectric.com*

Abstract

Although the mathematics for defining field weakening expressions are relatively uncomplicated, the application of these expressions for practical field-weakening implementations is not well documented. This paper describes the derivation of simplified expressions for implementing field weakening in field-oriented control (FOC) algorithms for use in a high torque, permanent-magnet synchronous motor designed for automotive in-wheel applications. The formulae are based on modelled motor characteristics and take into account the varying states of the system in terms of rotational speed, torque demand, and supply voltage to produce a few uncomplicated expressions. The simplicity of the calculations makes them appealing for use in microcontroller applications, where a high processing overhead is already taken up with current control and safety-critical functionality.

Keywords: field weakening, permanent magnet motor, control system

1 Introduction

Permanent magnet synchronous motors (PMSMs) are increasingly used in electric and hybrid vehicle traction applications due to their high starting torque and high torque density. In order to maximise overall motor efficiency, these motors are designed with typical drive-cycle data in mind, and so motor characteristics are chosen such that the highest efficiency occurs in the region of maximum duty of the torque-speed profile.

Since PMSMs produce back-EMF, and considering the maximum vehicle battery voltage, this design for efficiency may restrict the maximum speed of the vehicle. In order to operate in an extended speed range, without requiring additional gearing – such as in direct-drive applications – the motor control software is required to adopt a field-weakening strategy. In PMSM software using a field-oriented control

(FOC) method, this is achieved by controlling both direct and quadrature components of the stator current.

As a motor rotates, it creates a back-EMF voltage across its coils proportional to the speed of rotation. In order to force current into the coils, the applied voltage must exceed this voltage.

The limitation comes when the speed of rotation is such that the required applied voltage is greater than the voltage available from the inverter electronics. At this point, the inverter can no longer supply current to the stator coils and the motor will not generate any torque. If the rotor is externally forced to rotate faster, the back-EMF voltage will exceed the power supply voltage, and current will attempt to flow from the coils into the power supply, producing a torque counter to the direction of rotation.

In practical terms, this means that for a given power supply voltage, and a required coil current, there is a maximum speed of rotation obtainable before inverter saturation occurs preventing more

coil current from flowing into the coil. This speed is referred to as the base speed.

In order to exceed the base speed, the back-EMF voltage must be reduced. Since the back-EMF is also a function of the magnetic flux between rotor permanent magnets and stator coils, reducing this magnetic flux will reduce the back-EMF voltage. The inverter then does not enter saturation, current can flow into the stator coils, and the motor can rotate faster, although at the expense of reduced maximum torque.

The basic principle of field weakening, as its name suggests, is to weaken the magnetic field strength of the rotor magnets, by applying an opposing magnetic field on the stator coils in phase with the rotor field. This is the direct axis (d-axis) in field oriented control, and acts to reduce the back EMF generated by the motor as it rotates.

Since any practical vehicle battery voltage will vary with its state of charge over a drive cycle, along with a varying torque (and hence current) demand including regenerative braking, these must also be considered in the equations.

2 Calculating Base Speed

Here base speed is defined as the maximum speed at which rated current can be achieved at a given supply voltage, with no field weakening. This is the point at which the phase voltage required to produce rated current is equal to the available supply voltage. Using the FOC motor equations in the d-q plane:

$$V_d^2 + V_q^2 = V_{limit}^2 \quad (1)$$

In the steady-state:

$$V_d = I_d R - \omega_e L_q I_q \quad (2)$$

$$V_q = I_q R + \omega_e L_d I_d + \omega_e \psi_m \quad (3)$$

where ω_e is the electrical speed in rads^{-1} , L_d and L_q are phase inductances in Henries in the d and q axes, R is phase resistance in ohms, ψ_m is back-EMF constant in V s/rad, and I_q is coil current in the q-axis up to the maximum rated coil current. I_d is the field weakening current in the d axis.

Assuming a PWM strategy is adopted to maximise available applied voltage without over-modulation:

$$V_{limit} = \frac{V_{batt}}{\sqrt{3}} \quad (4)$$

Substituting for V_d and V_q in equation (1) using (2) and (3) and setting $I_d = 0$ to obtain the limit at base electrical speed ω_b in rads^{-1} before field weakening is applied, gives:

$$(-\omega_b L_q I_q)^2 + (I_q R + \omega_b \psi_m)^2 = V_{limit}^2 \quad (5)$$

Solving this for the base electrical speed ω_b produces a quadratic, whose solutions are:

$$\omega_{b(\text{motoring})} = \frac{-b + \sqrt{b^2 - 4ac}}{2a} \quad (6)$$

$$\omega_{b(\text{braking})} = \frac{-b - \sqrt{b^2 - 4ac}}{2a} \quad (7)$$

where $a = \psi_m^2 + (L_q I_q)^2$, $b = 2\psi_m I_q R$, and $c = (I_q R)^2 - V_{limit}^2$.

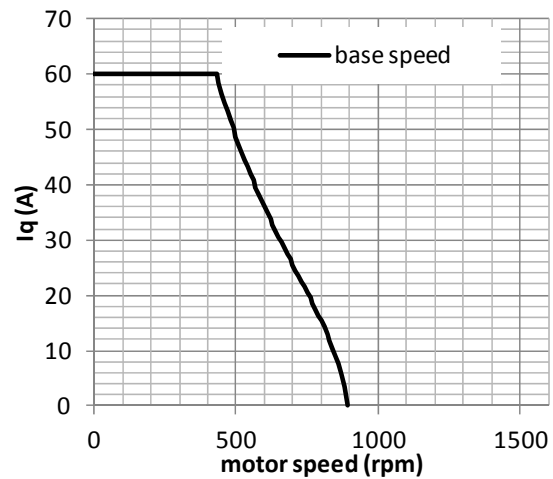


Figure 1: Maximum currents against speed without field weakening

Figure 1 shows how the maximum I_q must decrease as speed (converted to RPM) increases for an example motor in motoring mode using (6).

Table 1 Motor electrical parameters

Parameter	Value
R	0.210 Ohms
L_d	1.90 mH
L_q	1.77 mH
ψ_m	61.85 mV s/rad
N	32 rotor pole-pairs
V_{batt}	320 V
I_{rated}	60 A
$I_{continuous}$	32 A

At the point where I_q reaches zero amps, the generated back EMF equals the maximum voltage available from the inverter electronics. Table 1 shows the parameters for this motor.

2.1 Approximating Base Speed

By repeating the plot shown in Figure 1 across a range of battery voltages, it can be seen that the I_q current limit curve can be approximated as a straight line between the maximum speed at which I_q can achieve rated current (base speed) and the speed at which I_q equals zero as shown in Figure 2. By modifying (4), a margin of error can be applied to ensure that the real base speed is not exceeded, considering factors such as maximum PWM duty cycle and IGBT voltage drop.

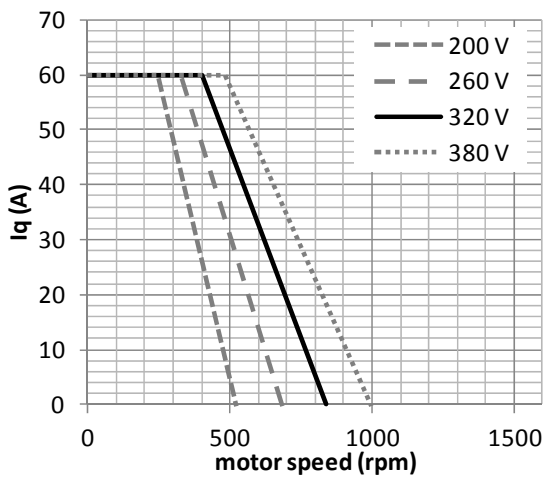


Figure 2: Approximated base speed lines at different battery voltages

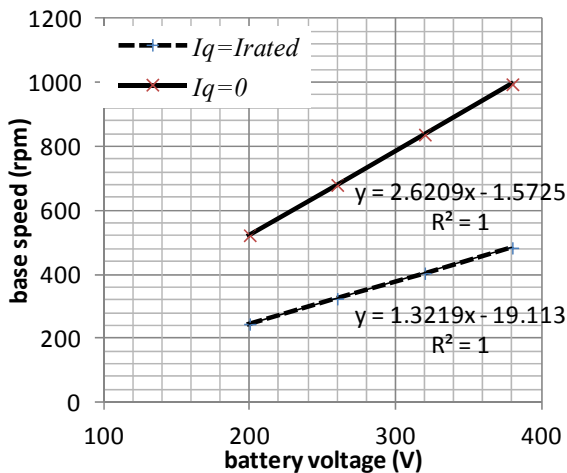


Figure 3: Base speeds as a function of battery voltage

Figure 3 shows the base speeds for rated current and zero current plotted against V_{batt} . It can be seen that these base speeds are linear functions of V_{batt} . These functions can be calculated for a particular design of motor to produce four constants that describe the base speed of that motor. In this example, in motoring mode, the constants become:

Table 2 Motoring field weakening constants

<i>constC1</i>	<i>constC2</i>	<i>constC3</i>	<i>constC4</i>
1.3219	-19.113	2.6209	-1.5725

The values in Table 2 are the gradients and y-intercepts of the lines in Figure 3.

3 Calculating Current Demands in the D and Q Axes

3.1 Field Weakening Strategy

The field weakening implementation considered in this paper for its simplicity is termed CVCP (constant voltage, constant power) [1]. This strategy allows the vector sum of the d and q axis voltages to reach the limiting voltage, and then remain there by controlling the d and q axis current demands.

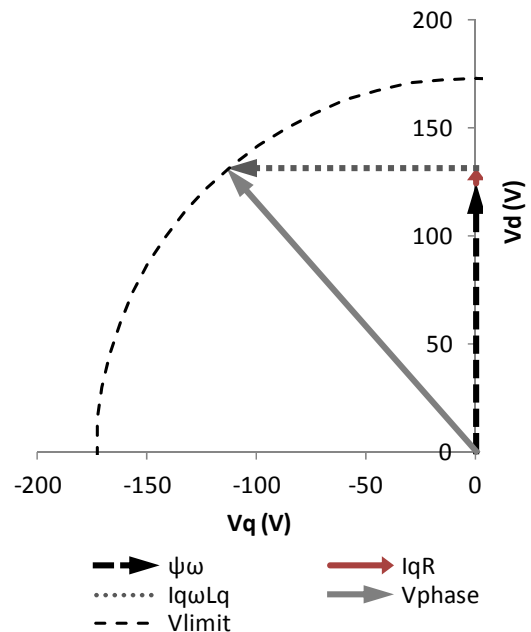


Figure 4: Voltages in the d and q axes

Figure 4 shows the individual voltage components of equations (2) and (3), and their vector sum V_{phase}

as it approaches the limiting voltage as per equation (1). It can be seen that the resistive components of the voltages are small in comparison with the inductive and back EMF terms, and so shall be ignored for simplicity when deriving the expressions for CVCP from equations (2) and (3) as follows:

$$\begin{aligned} V_d &= -\omega_e L_q I_q = -\omega_b L_q I_{rated} = constant \\ \rightarrow I_q &= I_{rated} \left(\frac{\omega_b}{\omega_e} \right) \end{aligned} \quad (8)$$

$$\begin{aligned} V_q &= \omega_e L_d I_d + \omega_e \psi_m = \omega_b \psi_m = constant \\ \rightarrow I_d &= -\frac{\psi_m}{L_d} \left(1 - \frac{\omega_b}{\omega_e} \right) \end{aligned} \quad (9)$$

since the resistive terms are assumed to be zero, and $I_d = 0$ at the limit of field weakening, ω_b .

3.2 Defining Speeds for Calculation

Speeds in RPM will be denoted by Ω . Figure 5 shows the limited d-q current demands with this field weakening strategy for an $I_{q(demand)}$ of 32 A, and defines the speeds required for calculating them, described in Table 3:

Table 3 Field weakening speed descriptions

Speed	Description
Ω_{A1}	Base speed for rated Iq current
Ω_{A2}	Base speed for zero Iq current
Ω_B	Base speed for demanded Iq current
Ω_C	Speed at which Iq demand reaches maximum q-axis current when field weakening

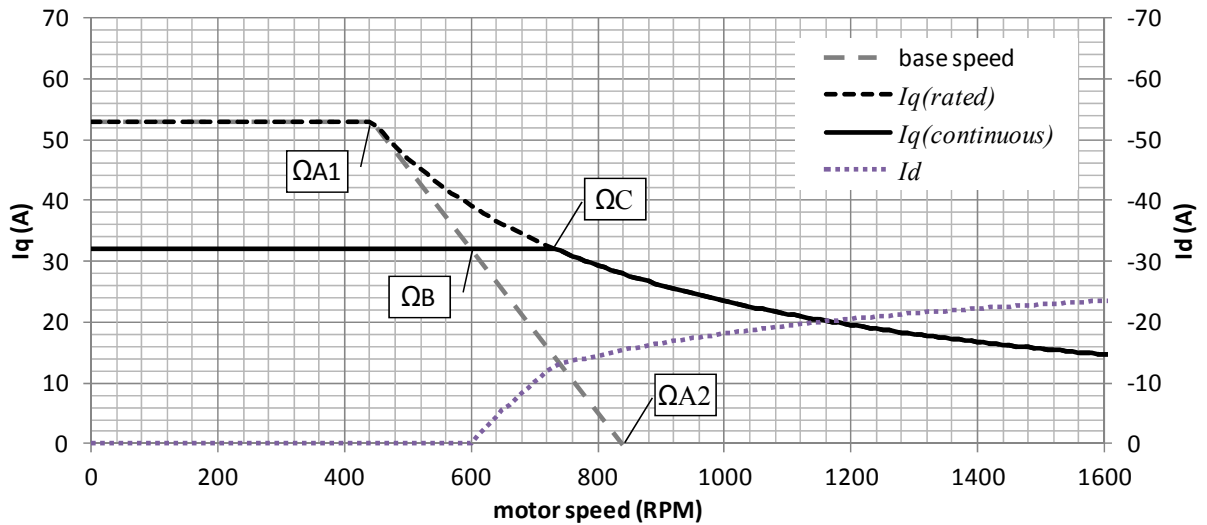


Figure 5: Definition of speeds for field weakening calculations

Referring to the constants in Table 2, the speed calculations can now be performed by the controller software as follows:

$$\Omega_{A1} = (constC1 \cdot V_{batt}) + constC2 \quad (10)$$

$$\Omega_{A2} = (constC3 \cdot V_{batt}) + constC4 \quad (11)$$

$$\Omega_B = \Omega_{A1} + (\Omega_{A2} - \Omega_{A1}) \cdot \left(1 - (I_{q(demand)}/I_{q(rated)}) \right) \quad (12)$$

$$\Omega_C = \Omega_{A1} (I_{q(rated)}/I_{q(demand)}) \quad (13)$$

The back EMF constant ψ_m is converted into volts per RPM and is denoted as K :

$$K = \frac{2\pi N \psi_m}{60} \quad (14)$$

Now the d-q currents I_d and I_q can be calculated:

$$\begin{aligned} \text{For } \Omega < \Omega_B, \\ I_d &= 0, \\ I_q &= I_{q(demand)} \end{aligned} \quad (15)$$

$$\begin{aligned} \text{For } \Omega_B \leq \Omega < \Omega_C, \\ I_d &= -\frac{K}{L_d} \left(1 - \frac{\Omega_B}{\Omega} \right) \left(\frac{\Omega_C - \Omega_{A1}}{\Omega_C - \Omega_B} \right) \\ I_q &= I_{q(demand)} \end{aligned} \quad (16)$$

$$\begin{aligned} \text{For } \Omega_C \leq \Omega, \\ I_d &= -\frac{K}{L_d} \left(1 - \frac{\Omega_{A1}}{\Omega} \right) \\ I_q &= I_{q(rated)} \left(\frac{\Omega_{A1}}{\Omega} \right) \end{aligned} \quad (17)$$

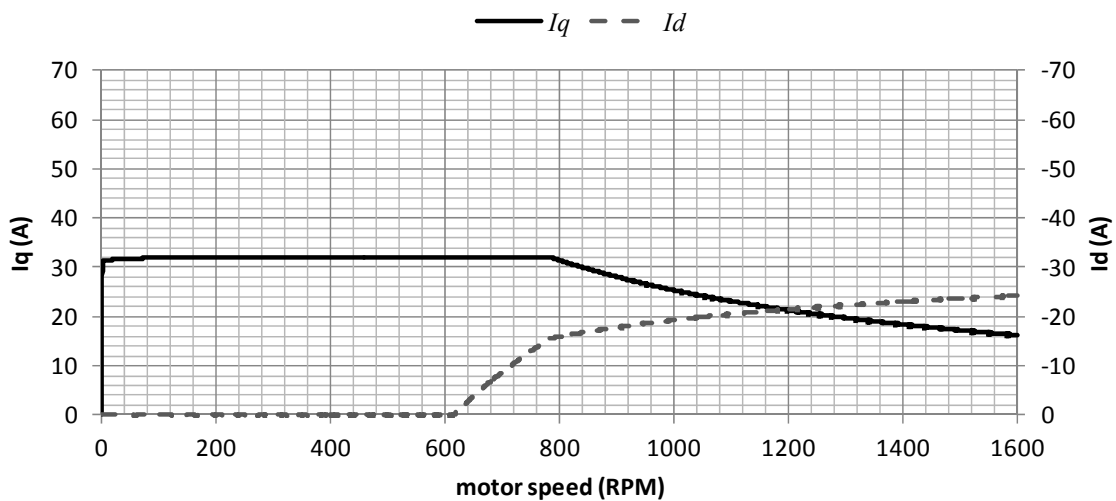


Figure 6: Simulated currents in d and q axes as a function of speed

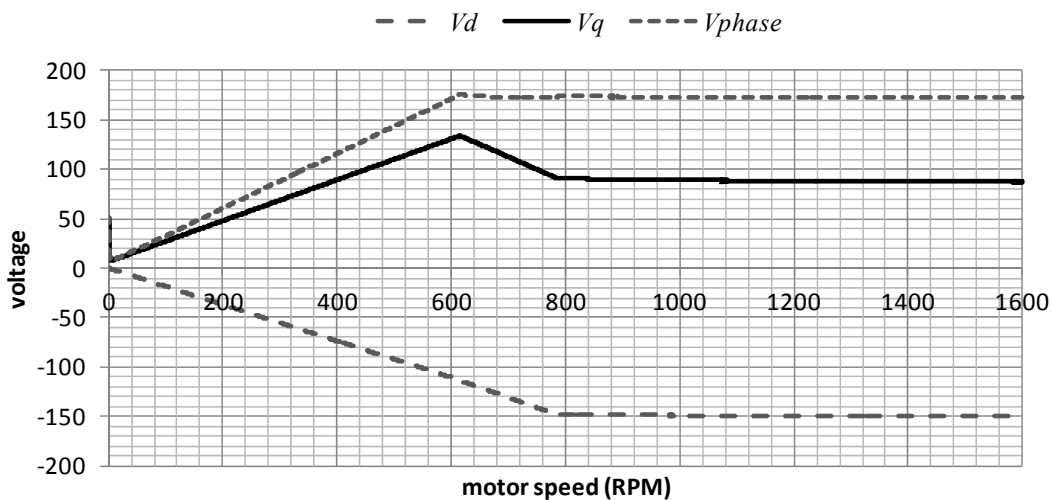


Figure 7: Simulated voltages in d and q axes as a function of speed

Simulation Results

Figures 6 and 7 show the simulation results from Simulink for this implementation using an electrical model of the example motor. The voltages in the d-q axes (V_d , V_q) are shown along with their vector sum (V_{phase}). For this simulation, $I_q(demand)$ is set at 32A, and V_{batt} is 320V. The field weakening limit (V_{limit}) is set to 94 % of the absolute voltage limit ($V_{batt}/\sqrt{3}$) to account for a practical limit in maximum attainable phase voltage due to IGBT forward voltage drop and a limitation in minimum PWM pulse width, as well as allowing a small margin

for variations in motor characteristics with temperature and stator core saturation.

The results in Figure 6 show the currents in d and q axes being controlled to the demands supplied by equations (15) through (17). Figure 7 shows how the magnitude of the voltage vector V_{phase} increases with speed until the base speed is reached at 620 RPM, and then remains approximately constant at (V_{limit}), as predicted by equation (1).

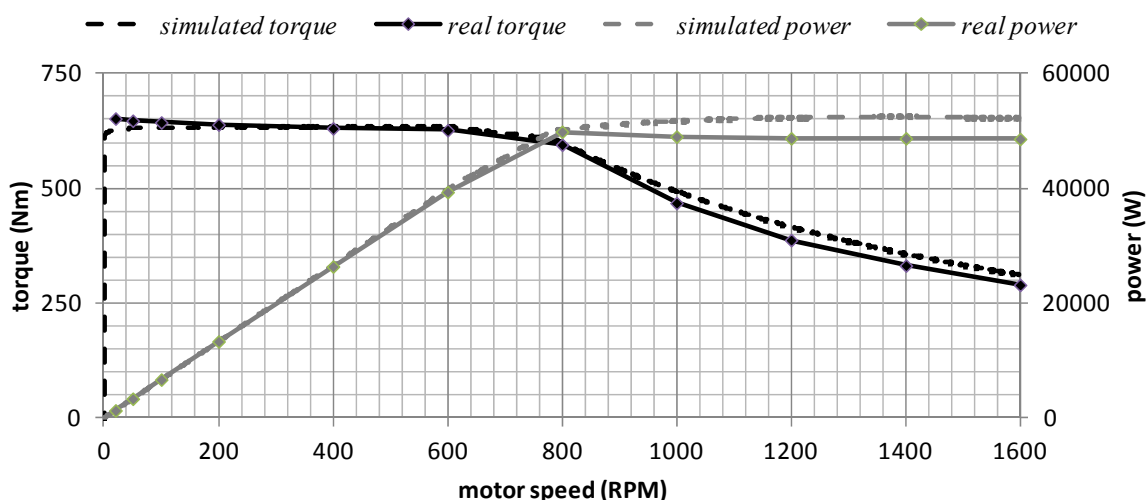


Figure 8: Real and simulated output torque and power as a function of speed

4 Experimental Results

This simplified field-weakening approach has been tested using an in-wheel motor with the electrical properties in Table 1. Robust PI loops are used to control current in the d and q axes to the demands supplied by equations (15) through (17). This motor (see Figure 9) consists of 8 individually controlled inverters, each providing an eighth of the total motor torque and having a torque constant of approximately 2.52 Nm/A. Thus, a 32A I_q demand to each inverter results in approximately 645Nm of total motor torque below base speed.



Figure 9: Protean in-wheel motor

Figure 8 shows the torque and mechanical power from the simulations, together with measured results from the motor under test, on a four-

quadrant dynamometer. The motor is supplied with a coolant temperature regulated at 50°C, and a flow rate of 15 litres/minute. The results show good correlation with the simulation, although deviation is observed as the temperature of the motor increases as the test progresses.

It is reasonable to attribute this to a reduction of the permanent magnet field strength with temperature, resulting in a reduced back EMF, and hence torque constant. Other factors to consider are an increase in coil resistance, and a change in stator core saturation with coil current, since these will also contribute to a reduction in flux linkage, and thus torque.

In particular, the results show the approximately constant power during field weakening, as predicted by equations (8) and (9).

5 Conclusions

The simplicity of the calculations make them appealing for use in small controller applications, where field weakening is required for motoring in an extended speed range. Expressions for regenerative braking can be derived in exactly the same way by using equation (7) to define the constants in Table 2.

There are some assumptions that should be made clear, however. Firstly, equations (8) and (9) have assumed that the phase series resistance is negligible. Secondly, due to the difference between L_d and L_q , the torque output will not remain flat as the I_q demand remains constant in the field weakening region (between Ω_B and Ω_C in Figure 5). Thirdly, the L_d and L_q inductances will



Figure 10: Protean demonstration vehicle

change with phase current due to core saturation, as will the flux linkage constant. This technique has been successfully demonstrated both in the laboratory and on the road (see Figure 10).

References

- [1] D.S Maric, S.Hiti, C.C.Stancu, J.M.Nagashima, "two flux weakening schemes for surface mounted permanent magnet synchronous drive-Design and transient response considerations", 1999.
- [2] Austin Hughes, "Electric Motors and Drives", third edition, 2006.
- [3] Gerd Terörde, "Electric Drives and Control Techniques", second edition, 2009.

Authors



Tim Martin received his bachelors' degree in electronic engineering from the University of Southampton in 1992. Originally from an electronic design background for motor drives in precision positioning systems, and embedded software for electric vehicle control systems, he has been a Principal Software Engineer for Protean Electric Limited since 2008.



Richard Burke was awarded a first class degree from Keble College, Oxford University in 1984. Since then he has worked in a variety of engineering industries including aero-engines at Rolls Royce, ticketing systems at Cubic Transportation, automotive diagnostics at Omitec Limited and in-wheel electric motors with his current employer, Protean Electric Limited in Farnham, UK. His current position is Senior Software Manager in charge of developing the software for Protean's electric wheel motors, a role he has held for the last 4 years. He is a chartered engineer and a member of the IET.